생활과학석사학위논문

In Silico Prediction of Competitive Inhibitory Activities of Terpenes against 5α-Reductase Type 2

컴퓨터 시뮬레이션에 의한 Terpene류의

5α-Reductase Type 2에 대한 경쟁적 저해능 예측

February 2019

서울대학교 대학원

식품영양학과

김 륜 희

ABSTRACT

In Silico Prediction of Competitive Inhibitory Activities of Terpenes against 5α-Reductase Type 2

Ryun-Hee Kim

Department of Food and Nutrition

The Graduate School

Seoul National University

5α-Reductase type 2 (5αR2) catalyzes the reduction of testosterone to dihydrotestosterone (DHT) in scalp hair follicles. Increased intracellular DHT is responsible for development of androgenetic alopecia (AGA), or male-pattern hair loss. Thus, inhibition of 5αR2 activity is important to retard progression of AGA. Terpenes, metabolites produced by diverse plant sources, have been suggested to have enhancing effects on hair growth. The aims of the present study were to predict 3D structure of 5αR2, which has not been yet reported, and to determine which terpene could have competitive inhibitory activity against NADPH or testosterone binding site of 5αR2 by *in silico* approaches.

Prior to performing molecular docking of terpenes to 5αR2, 3D structure of

5αR2 was predicted by I-TASSER server. Discrimination ability of a docking protocol was validated by receiver operating characteristic curve analysis. By molecular docking of 577 terpenes from NuBBE database to the predicted 3D structure of 5αR2 using AutoDock Vina, 18 triterpenoids were predicted to have lower binding energies than NADPH against 5αR2. 247 out of 577 terpenes were predicted to have lower binding energies than testosterone against 5αR2. Among these 247 terpenes, 3 triterpenoids were predicted to have lower binding energies than finasteride and dutasteride, well-known competitive inhibitors of 5αR2. In conclusion, triterpenoids having a steroid ring or pentacyclic ring in backbone were predicted to have the highest competitive inhibitory activities than monoterpenoids, iridoids, sesquiterpenoids, diterpenoids, and steroids against 5αR2.

Keywords: 5α-Reductase type 2; Androgenetic alopecia; Molecular docking; Competitive inhibitory activity; Triterpenoid

Student Number: 2017-29285

CONTENTS

LIST OF TABLES

LIST OF FIGURES

INTRODUCTION

5α-Reductase type 2 (5αR2) is an NADPH-dependent enzyme catalyzing conversion of testosterone to dihydrotestosterone (DHT) in androgen-sensitive tissues such as dermal papilla cells in scalp hair follicles.[1-3] Increased intracellular DHT level has been suggested to induce miniaturization of hair follicles and shortened duration of growth phase in hair follicle cycle, which eventually causes androgenetic alopecia (AGA) or male-pattern hair loss.[4,5] In addition, it was reported that men who are genetically deficient in 5αR2 do not have receding hairlines at temporal scalp regions.[6] Hence, in order to prevent or delay progression of AGA, it is crucial to decrease intracellular DHT level via inhibition of 5αR2 activity.

Currently, two synthetic 4-azasteroidal compounds, finasteride and dutasteride, have been known as competitive inhibitors of 5αR2.[7,8] Finasteride, sold under the brand names Proscar and Propecia, has been approved by US Food and Drug Administration (FDA) for use in AGA treatment.[9] Dutasteride, sold under the brand name of Avodart, was originally approved by US FDA for treatment of benign prostatic hyperplasia (BPH)[10] and previous clinical studies demonstrated that administration of dutasteride was effective in increasing the number of hair in men with AGA.[11-13] Nevertheless, it has been reported that long-term administration of finasteride and dutasteride could cause some side effects such as decreased libido, ejaculatory dysfunction, and erectile dysfunction.[14]

Whether non-synthetic substances from plant sources can have treatment effects on AGA has been studied as well. For example, extracts of *Eclipta alba*,[15] leaves of

Acanthopanax koreanum,[16] red ginseng,[17] and *Lycopersicon esculentum*[18] were reported to be effective in enhancing hair growth. All these four extracts contain eclalbatin, acankoreoside J, ginsenoside R_0 and Rg_3, and lycopene, respectively, which belong to terpenes. Given these facts, it could be hypothesized that other terpenes would have promoting effects on hair growth as well, and their effects would be quantitatively different depending on their distinct structural characteristics such as the number of isoprene unit in backbone and types of side-chains.

Molecular docking is a widely used computational approach that simulates binding of ligands to a target protein. It characterizes bound conformations of the ligands within a binding site and binding affinities of the ligands toward the protein.[19] In order to virtually screen which structural classes of terpenes are most likely to inhibit 5αR2 activity, molecular docking was employed in this study. Especially, competitive inhibitory activities of terpenes against 5αR2 were predicted in this study, in which it could be elucidated which individual terpene had higher binding affinity than NADPH or testosterone for the same binding sites via molecular docking. Since three-dimensional (3D) structure of 5αR2 has not been yet reported, it is essential to predict its 3D structure to perform molecular docking. Thus, the 3D structure of 5αR2 was predicted by *in silico* modeling prior to the virtual screening (VS) in the present study. The overall purpose of this study was to quantitatively predict competitive inhibitory activities of different structural classes of terpenes against 5αR2 by molecular docking based on the predicted 3D structure of 5αR2.

METHODS

1. Prediction of 3D Structure of 5αR2

Sequence identity of 5αR2 was analyzed by PSI-BLAST search,[20] by which it was figured out that 5αR2 had a sequence identity below 30% with proteins in Protein Data Bank (PDB).[21] However, it was not enough to be informative to identify template proteins likely to come from a common evolutionary origin as 5αR2. Accordingly, a 3D structure of 5αR2 was predicted by fold recognition and *ab initio* modeling approaches regardless of evolutionary relationships between 5αR2 and other proteins in PDB.

Based on amino acid sequence of 5αR2 provided by UniProt (UniProt ID: P31213),[22] the 3D structure of 5αR2 was predicted by iterative threading assembly refinement (I-TASSER) server, a suite containing several programs for structural prediction based on fold recognition and *ab initio* modeling approaches.[23,24] Sequence alignments were conducted by PSI-BLAST search embedded in I-TASSER server,[24] by which 5αR2 sequence was divided into aligned and unaligned regions. It was determined by whether the region had the same fold as a part of any other proteins in PDB. LOMETS, a set of fold recognition programs embedded in I-TASSER server, was applied in recognizing template proteins to be used for modeling aligned regions in 5αR2 sequence.[24] From PDB, chain A of Δ^{14}-sterol reductase (PDB ID: 4QUV)[25] and isoprenylcysteine carboxyl methyltransferase (PDB ID: 5V7P)[26] were selected as template proteins which were recognized to have most likely the same fold as 5αR2 regardless of how closely they have evolutionary relationships with 5αR2. Structures of unaligned regions in 5αR2

sequence were built by *ab initio* modeling. By reassembling structures of the template proteins identified by fold recognition and structures produced by *ab initio* modeling, a predicted 3D structure of 5αR2 was generated, which was named as apo-5αR2 in this study.

2. Construction of a Binary Complex of the Apo-5αR2 with NADPH

Structural file of NADPH was downloaded from PubChem (PubChem CID: 5884)[27] and converted to PDBQT format required for molecular docking by Open Babel.[28] Since NADPH binding site of 5αR2 has not been clear, a blind docking was performed to predict NADPH binding site in the apo-5αR2 without designating specific residues. Center of the docking box was set to x= 63.1734, y= 62.4446, and z= 62.8212; and size of the docking box was set to 60 Å *66 Å * 60 Å, which was large enough to cover whole structures of the apo-5αR2.

Consequently, 9 different binding poses (binding modes) of NADPH were predicted. Among 9 binding modes of NADPH, only one was selected by the criteria of whether it had the lowest binding energy and whether surrounding regions of NADPH binding site formed a pocket-like structure. From the selected binding mode of NADPH, amino acids involved in binding with NADPH were characterized, and surrounding regions of these amino acids were considered as predicted NADPH binding site. At the predicted NADPH binding site, 3D structure of NADPH was combined with the apo-5αR2 as a single enzyme model in PDB format using copy/combine function of UCSF Chimera.[29] This binary complex was named as holo-5αR2 in this study.

3. Structural Validation of the Apo-5αR2

Reliability of the apo-5αR2 was assessed using web-servers (PROCHECK,

ProSA, and ERRAT) that computed any potential structural errors based on structural information of proteins whose structures have already been experimentally determined. Ramachandran plot of the apo-5αR2 provided by PROCHECK[30] was used to examine whether backbone dihedral angles (phi and psi angles) in a polypeptide chain of the apo-5αR2 were stereochemically possible. ProSA[31] was used to evaluate conformation and corresponding potential energy of the apo-5αR2. ProSA calculated z-score which measures deviation of the potential energy of the apo-5αR2 with respect to potential energy distribution of all possible conformations of 5αR2.[31] ERRAT[32] was used to assess non-covalently bonded atomic interactions between amino acids in the apo-5αR2. ERRAT calculated an error value for every amino acid and overall quality factor of the apo-5αR2.[32] Overall quality factor of the apo-5αR2 was expressed as a percentage of amino acids whose error values were below 95% confidence limit out of total amino acids in the apo-5αR2.

4. Validation of a Docking Protocol by Receiver Operating Characteristic (ROC) Curve Analysis

Discriminability of the docking protocol of this study was validated by ROC curve analysis[33] using SPSS 23.0 software (SPSS Inc., Chicago, IL, USA). The docking protocol referred to a workflow of predicting binding affinities of compounds toward the predicted 3D structure of 5αR2 using AutoDock Vina.[34]

In order to plot the ROC curve, active and inactive ligand data sets were obtained from ChEMBL database[35] and DUD-E server,[36] respectively. In detail, 470 molecules with IC_{50} values for 5αR2 were provided by ChEMBL database (ChEMBL ID: ChEMBL1856). Among these 470 molecules, 202 molecules with

IC_{50} values below 7 nM were selected. This IC_{50} value was the same as that of dutasteride, which was used as a reference molecule of this study.[37,38] Tanimoto coefficients were calculated using Open Babel. Structural similarities between these 202 molecules were judged by the Tanimoto coefficients. The active ligand data set was shortlisted on the basis of the Tanimoto coefficient cut-off value (0.5). Consequently, 149 molecules were selected and considered as active molecules. Based on these 149 active molecules, 669 decoys as inactive molecules were generated by DUD-E server. These 669 decoys were computed to have similar physical properties with those of active molecules in molecular weight, the number of hydrogen bond donors and acceptors, octanol-water partition coefficient, the number of rotatable bonds, and net molecular charge.[36] These decoys were presumed not to inhibit 5αR2 activity since they had dissimilar topologies with active molecules.[36] 149 active molecules and 669 decoys were docked to the holo-5αR2 using AutoDock Vina. Structural files in SDF format of 818 ligands were converted to PDBQT format by Open Babel. Center of the docking box was set to x =75, y =61, and z =75; and size of the docking box was set to 33 Å * 32 Å * 31 Å, which was large enough to cover the predicted testosterone binding site and surrounding residues. Docking parameters of AutoDock Vina were kept default.

Consequently, 9 different binding modes per active molecule or decoy were predicted. Only one binding mode of each active molecule or decoy was selected by the criteria of whether it had the lowest binding energy and whether its location was similar to that of testosterone. According to docking results (binding energies) of these 818 molecules (149 active molecules and 669 decoys), the ROC curve of the docking protocol was drawn based on sensitivity (true positive rate) and (1-

specificity) (false positive rate) of the docking protocol.

5. Preparation of Enzyme Models and Ligands

The apo-5αR2 and the holo-5αR2 were used as enzyme models for molecular docking. 577 structural files of terpenes isolated from plant sources (monoterpenoids, iridoids, sesquiterpenoids, diterpenoids, steroids, and triterpenoids) as target ligands were obtained from NuBBE database.[39] AutoDock Tools[40] was employed to convert the enzyme models in PDB format to PDBQT format. Open Babel was used to convert not only terpene structural files in MOL2 format to PDBQT format, but also structural files in SDF format of NADPH, testosterone (PubChem CID: 6013), finasteride (PubChem CID: 57363), and dutasteride (PubChem CID: 6918296) to PDBQT format.

6. Molecular Docking-Based VS of Competitive Inhibitory Activities of Terpenes against 5αR2

Two competitive inhibition mechanisms against 5αR2 were applied to molecular docking-based VS. One was competitive inhibition against NADPH binding site of 5αR2, which was designated as type A inhibition. The other was against testosterone binding site of 5αR2, which was designated as type B inhibition. AutoDock Vina was used to simulate molecular docking. Docking parameters of AutoDock Vina were kept default.

In order to virtually screen type A inhibitory activities of terpenes, 577 terpenes were docked to the predicted NADPH binding site in the apo-5αR2. The binding affinities of terpenes toward the apo-5αR2 were compared with that of NADPH. Center of the docking box for VS of type A inhibitory activities of terpenes was set to x= 67, y= 60, and z=64; and size of the docking box was set to 33 Å * 25 Å * 24

Å, which was large enough to cover the predicted NADPH binding site and surrounding residues.

Since testosterone binding site of 5αR2 has not been clear, the blind docking was performed to predict testosterone binding site in the holo-5αR2 without designating specific residues, prior to performing VS of type B inhibitory activities of terpenes. Testosterone was docked to the holo-5αR2 by blind docking via AutoDock Vina. Center of the docking box was set to x= 63.1734, y= 62.4446, and z= 62.8212; and size of the docking box was set to 60 Å * 66 Å * 60 Å, which was large enough to cover the whole structures of the holo-5αR2.

Consequently, 9 different binding modes of testosterone were predicted. Among 9 binding modes of testosterone, only one was selected by the criteria of whether it had the lowest binding energy, whether testosterone bound near the predicted NADPH binding site, and whether surrounding regions of testosterone binding site formed a pocket-like structure. From the selected binding mode of testosterone, amino acids involved in binding with testosterone were characterized, and surrounding regions of these amino acids were considered as predicted testosterone binding site.

577 terpenes were docked to the predicted testosterone binding site in the holo-5αR2. Finasteride and dutasteride were also docked to the same binding site as the reference molecules. The binding affinities of terpenes toward the holo-5αR2 were compared with those of testosterone, finasteride, and dutasteride. Center of the docking box for VS of type B inhibitory activities of terpenes was set to x =75, y =61, and z =75; and size of the docking box was set to 33 Å * 32 Å * 31 Å, which was large enough to cover the predicted testosterone binding site and surrounding

residues.

RESULTS AND DISCUSSION

1. Prediction of 3D Structure of 5αR2

In order to perform molecular docking, 3D structure of 5αR2 was needed. However, a crystal structure of 5αR2 is not experimentally determined so far, since 5αR2, an integral protein, is not stable enough to be purified.[1] Thus, a 3D structural model of 5αR2 was prepared by I-TASSER server. Initially, five 3D structural models of 5αR2 were predicted by I-TASSER server based on 5αR2 amino acid sequence. Among them, the model with the highest c-score (-0.64) was selected. The selected model was considered to have the most correct fold among the five models.[41] The selected predicted 3D structure of 5αR2 was named as apo-5αR2. The apo-5αR2 was predicted to be composed of 10 α-helix segments and 11 random coil segments (Figure 1). This result is consistent with that of a previous study in which hydrophobic transmembrane regions of integral membrane proteins mainly consist of α-helixes.[42]

2. Construction of a Binary Complex of the Apo-5αR2 with NADPH

The binary complex of 5αR2 with NADPH (holo-5αR2) was also constructed based on the fact that 5αR2 cannot be activated to convert testosterone to DHT until NADPH first binds to 5αR2.[43] By the blind docking, NADPH was predicted to be located inside the apo-5αR2 and close to c-terminal part of the apo-5αR2 (Figure 1). This result is consistent with those of other studies in which the c-terminal half of 5αR2 appears to be a NADPH-binding domain.[1,44] Also, 21 amino acids of 5αR2 (Trp53, Gln56, Tyr91, Arg94, Val97, Tyr98, Ser99, Leu100, Leu101, Leu111, Arg114, Gly115, Cys119, Asn160, Asp164, Arg168, Asn193, Glu197,

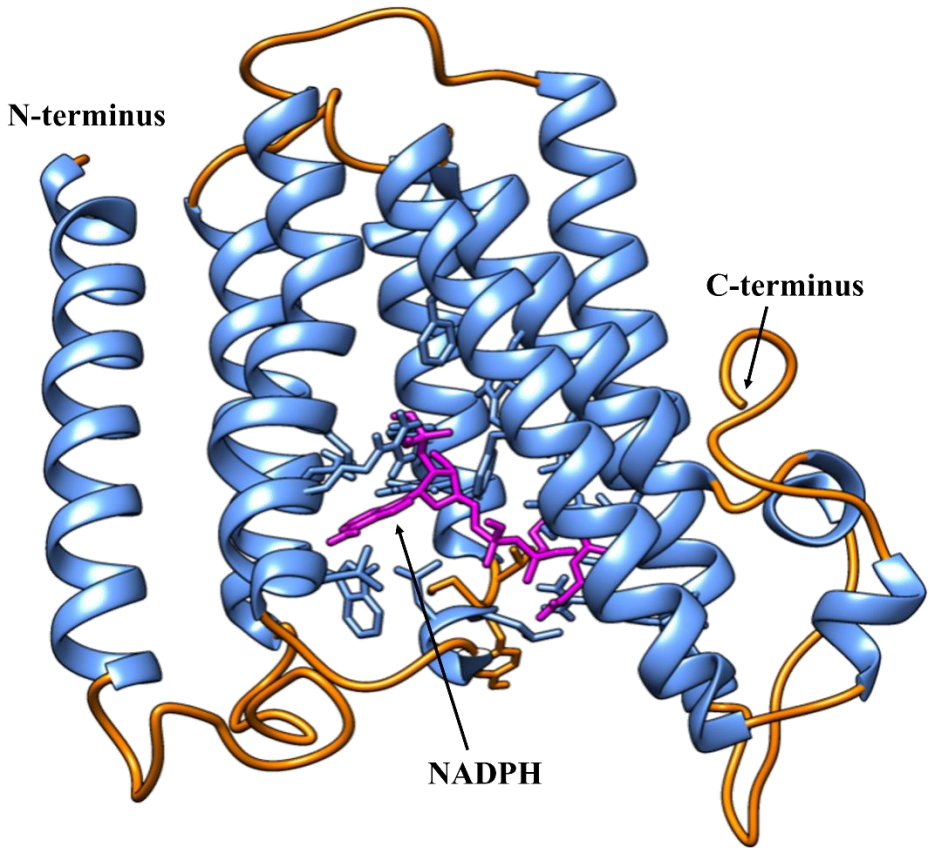

Figure 1. Predicted three-dimensional structure of 5α-reductase type 2.

Trp201, Phe223, and Arg227) were predicted to be involved in binding with NADPH. Surrounding regions of these amino acids were considered as predicted NADPH binding site. Among these 21 amino acids predicted to be involved in binding with NADPH, 6 amino acids (Tyr91, Leu100, Leu111, Arg114, Asn160, and Arg227) were identified to bind with NADPH via hydrogen bonding using UCSF Chimera.

3. Structural Validation of the Apo-5αR2

In Ramachandran plot of the apo-5αR2 provided by PROCHECK, 79.1% and 2.4% of 254 amino acids in the apo-5αR2 belonged to the most favored regions and disallowed regions, respectively (Figure 2). 79.1% of the amino acids in the apo-5αR2 are judged to have stable or highly stereochemically allowed conformations based on the fact that atoms of amino acids in the most favored regions do not have steric collisions between adjacent atoms.[45] Among 254 amino acids in the apo-5αR2, 5 amino acids (2.4%) are considered to have stereochemically unfavorable conformations based on the fact that atoms of amino acids in disallowed regions are disrupted by adjacent atoms.[45] However, since these 5 amino acids (Arg46, Ser74, Asp138, Leu170, and Ile176) were not in the region involved in binding with NADPH or testosterone, their conformations would not affect binding of ligands to the apo-5αR2 in a docking simulation. Also, it has been reported that Ser, Asp, and Arg have tendencies to adopt disallowed backbone conformations.[46,47] The z-score of the apo-5αR2 calculated by ProSA was -2.81, which was within the z-score range of native proteins having similar size with 5αR2 in PDB library (Figure 2). It has been known that z-score of any erroneous structural model would be outside the range of native proteins reported so far.[31]

PROCHECK

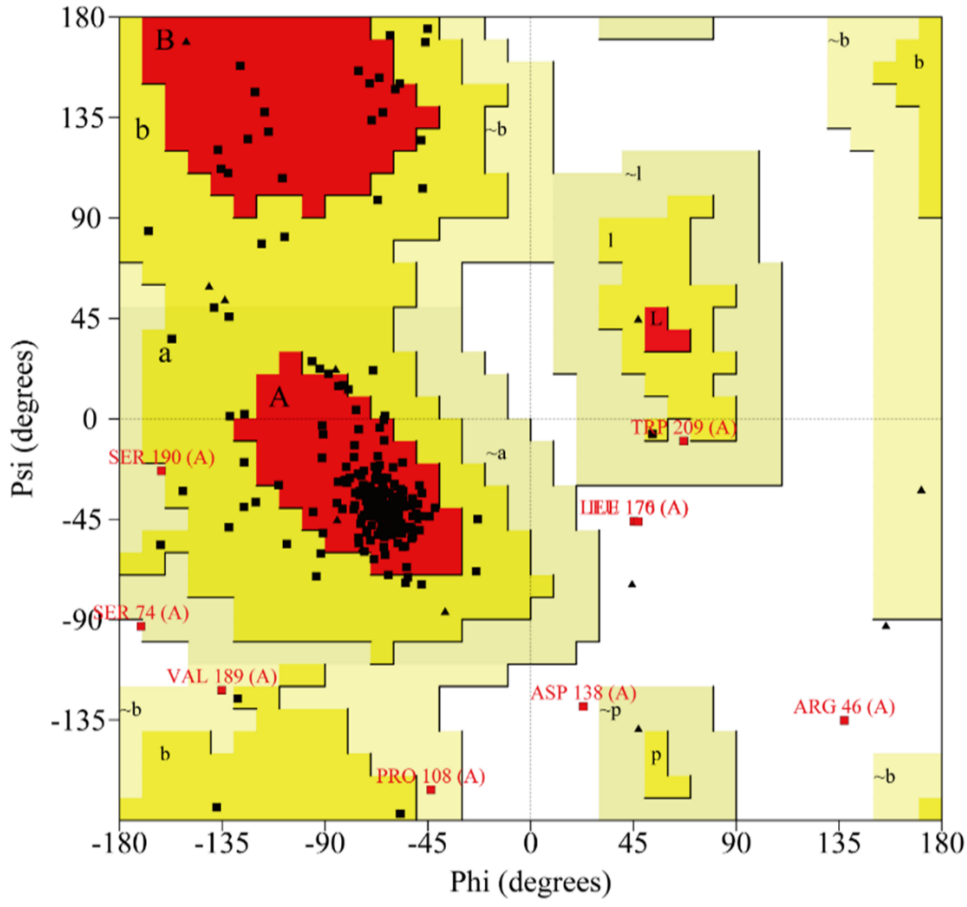
Psi (degrees)
Phi (degrees)
180
135
90
45
0
-45
-90
-135
-180
B
b
a
A
L
l
~b
~l
~a
~p
p
SER 190 (A)
SER 74 (A)
VAL 189 (A)
PRO 108 (A)
TRP 209 (A)
ASP 138 (A)
ARG 46 (A)

ProSA

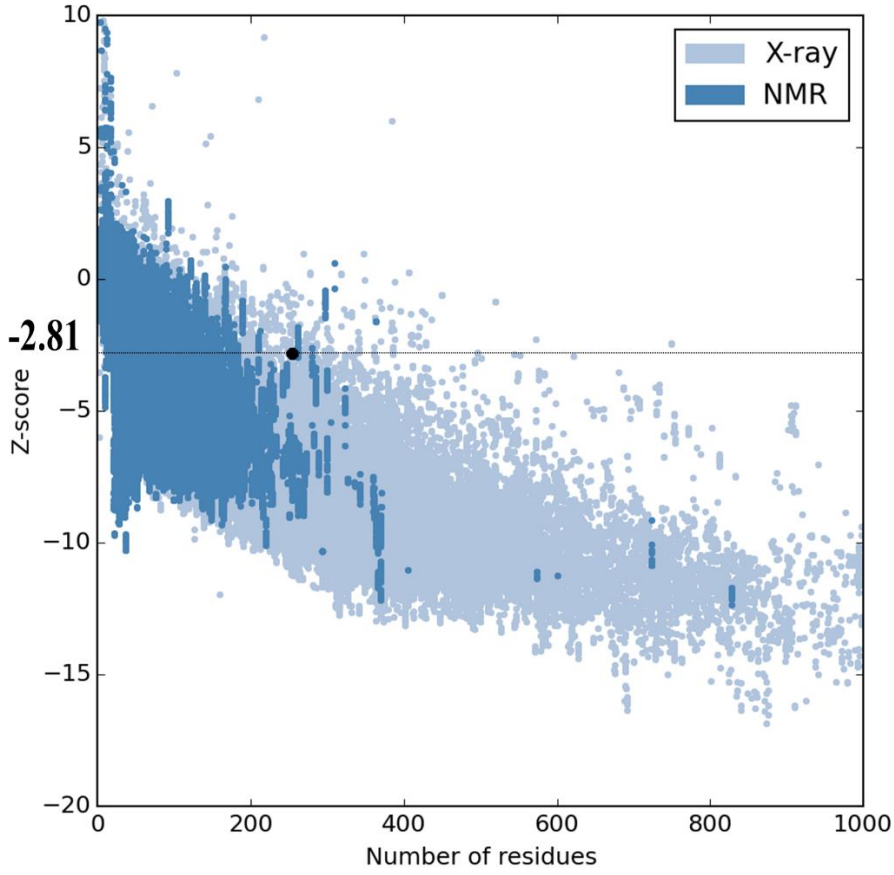
X-ray
NMR
-2.81
Z-score
Number of residues
10
5
0
−5
−10
−15
−20
0
200
400
600
800
1000

ERRAT

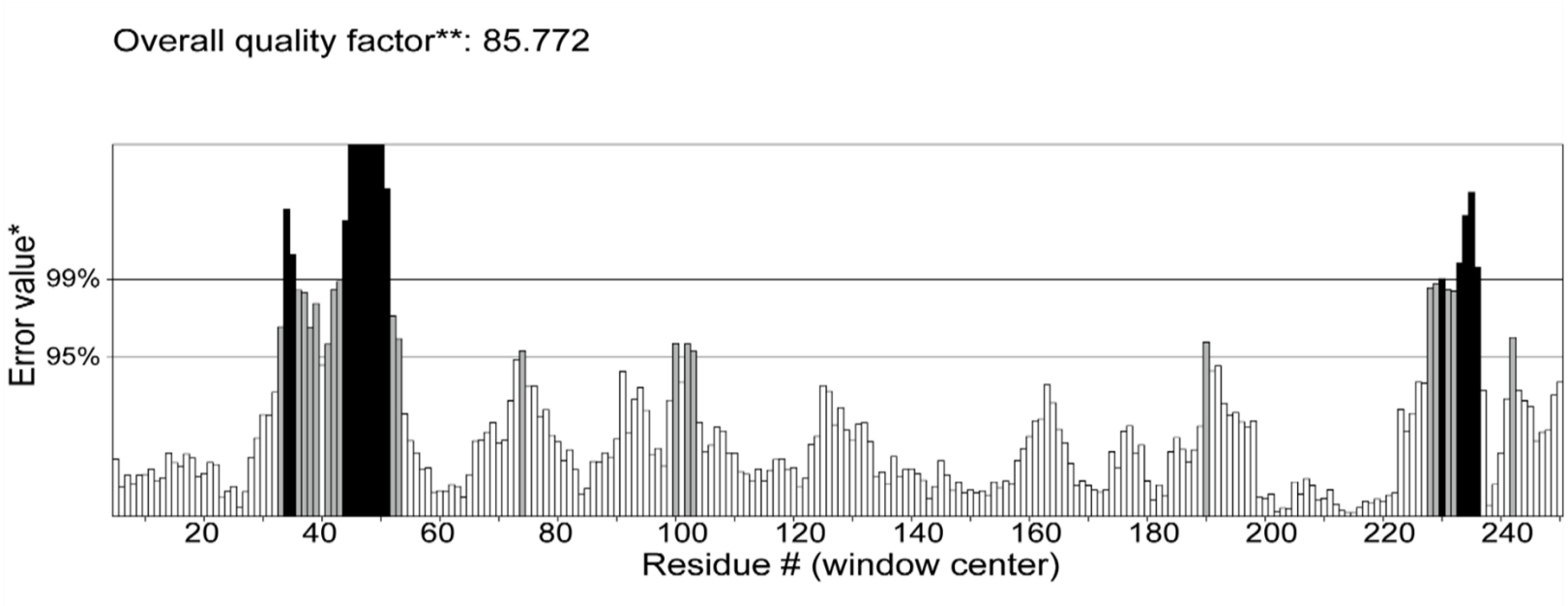

Figure 2. Structural validation of the predicted three-dimensional structure of 5α-reductase type 2.

Also, the z-score of the apo-5αR2 fulfilled that stable folds composed of 100-300 amino acids mostly have the negative values of z-scores.[48] Overall quality factor of the apo-5αR2 calculated by ERRAT was 85.772 (Figure 2). Amino acids with error values over 95% confidence limit have high probabilities that corresponding atoms would be misplaced.[32] Thus, the lower the number of amino acids with error values over 95% confidence limit, the higher overall quality factor of the model, which means that 85.772% of 254 amino acids of the apo-5αR2 are placed in appropriate regions based on their non-covalently bonded atomic interactions.[32] Collectively, these results of the structural validation indicate that the apo-5αR2 can be considered as an acceptable structural model of 5αR2 to be used in molecular docking. However, local conformations of the apo-5αR2 which have structural errors computed by PROCHECK and ERRAT would be further needed to be refined using molecular dynamics simulation.

4. Validation of the Docking Protocol by ROC Curve Analysis

The ROC curve analysis is used to assess discrimination ability of a diagnostic test, which has been also applied to evaluation of a VS workflow.[33,49] Accordingly, based on docking results of 149 active molecules and 669 decoys, the ROC curve of the docking protocol of this study was drawn (Figure 3). The ROC curve was above diagonal line, and the area under the ROC curve (AUC) was 0.781 (95% confidence interval, 0.744-0.817; p<0.0005), indicating 78.1% of probability that the docking protocol could select active molecules and discard decoys.[49] Also, the AUC of 0.7 to 0.8 implies that the docking protocol has an acceptable level of discrimination ability.[49]

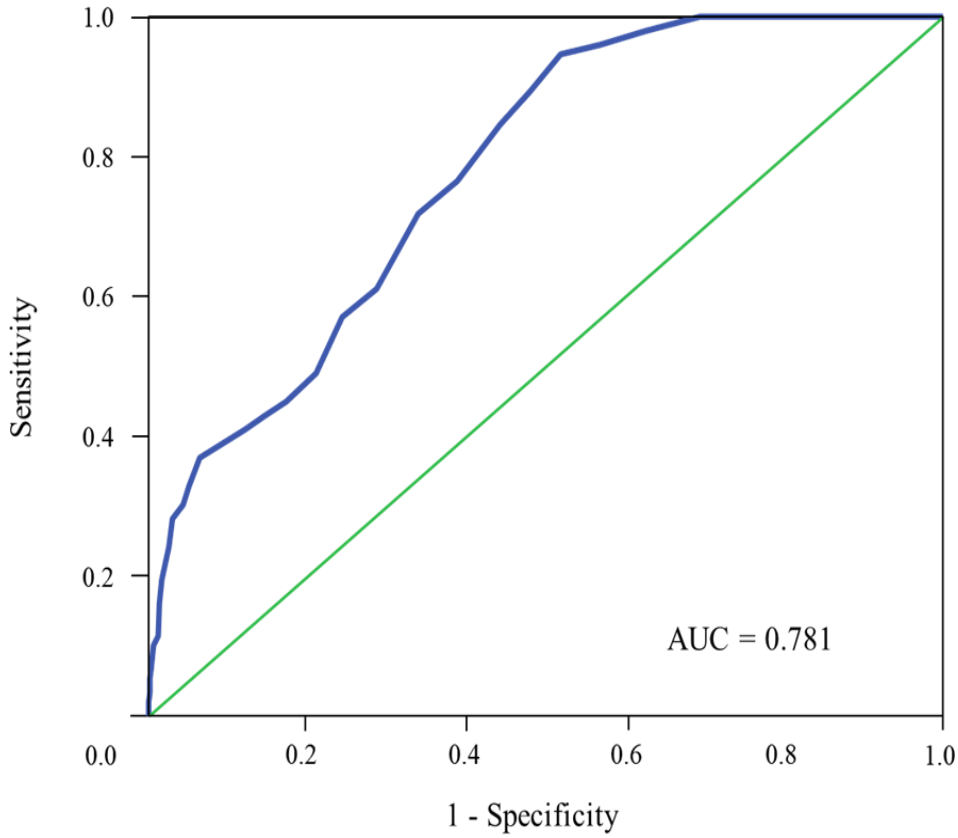

Figure 3. Receiver operating characteristic (ROC) curve of the docking protocol and the value of the area under the ROC curve (AUC).

5. Molecular Docking-Based VS of Competitive Inhibitory Activities of Terpenes against 5αR2

Following molecular docking-based VS using AutoDock Vina, the binding energy (ΔG, kcal/mol) of individual terpene was able to be compared with those of NADPH and testosterone as well as finasteride and dutasteride, well-known competitive inhibitors of 5αR2. The binding energies of ligands are inversely proportional to their binding affinities toward 5αR2, implying that the lower binding energies against 5αR2 ligands have, the stronger ligands are likely to bind to 5αR2, blocking other ligands not to bind to 5αR2.[50] Accordingly, it was able to be quantitatively determined which terpene could have competitive inhibitory activities against NADPH (type A) and testosterone (type B) binding sites of 5αR2, based on the calculated binding energies against 5αR2. Among 577 terpenes (monoterpenoids, iridoids, sesquiterpenoids, diterpenoids, steroids, and triterpenoids), 18 triterpenoids were calculated to have lower binding energies than NADPH (-10 kcal/mol) against its predicted binding site (Table 1). Namely, these 18 triterpenoids would be likely to have type A inhibitory activities, while monoterpenoids, iridoids, sesquiterpenoids, diterpenoids, and steroids would not. Among these 18 triterpenoids, 7 triterpenoids (21- and 23-hydroxycedrelonelide, cabraleone, nilocetin, nimbolin, shidasterone, and melianone) were noticed to have a steroid skeleton with a side-chain at C-16 or C-17 position. This result is supported by many synthetic steroidal inhibitors of 5αR2, including finasteride and dutasteride, having a bulky or lipophilic group at C-17.[51,52] In this regard, several quantitative structure-activity relationship studies on inhibitors of 5αR2 have reported that bulky side-chain substituted at C-17 of steroids can increase their

Table 1. Predicted binding energies (ΔG) and structural formulas of 18 triterpenoids predicted to have inhibitory activities against NADPH binding site of 5α-reductase type 2

Rank	Compound	NuBBE ID	ΔG (kcal/mol)	Structural formula
1	21-Hydroxycedreloneli de	1181	-11.5	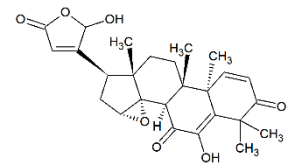
2	Celastrol	407	-11.1	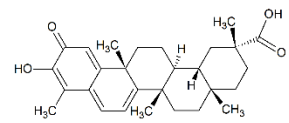
3	22β-Hydroxymaytenin	381	-10.9	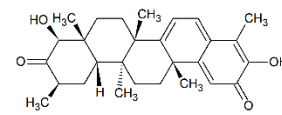
4	Netzahualcoyone	384	-10.6	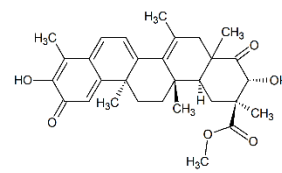
5	23-Hydroxycedreloneli de	1183	-10.5	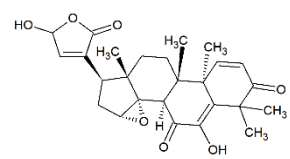
6	Cabraleone	1727	-10.5	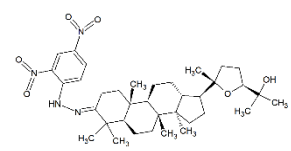
7	Nilocetin	1149	-10.4	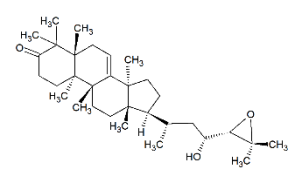

8	Netzahualcoyene	258	-10.4	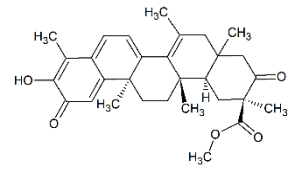
9	Netzahualcoyonol	382	-10.4	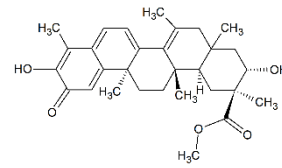
10	Compound T34389	-	-10.4	-
11	Nimbolin	1294	-10.3	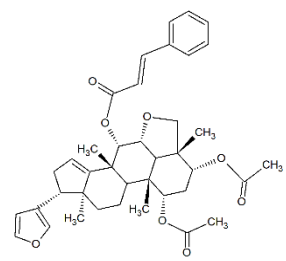
12	28-O-β-D-Glucopyranosyl ester of 29-hydroxyplatanic acid	1624	-10.3	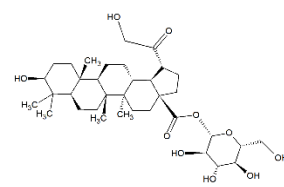
13	Jacoumaric acid	387	-10.3	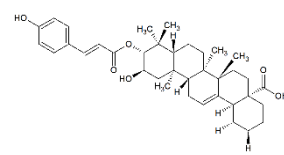
14	Compound T31900	-	-10.2	-
15	Shidasterone	1230	-10.1	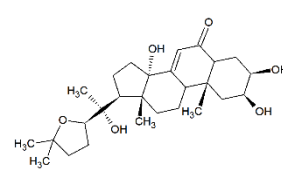

16	3β-Phenylacetoxyurs-12-ene	1347	-10.1	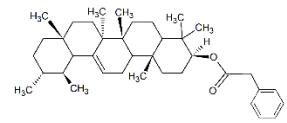
17	Melianone	1523	-10.1	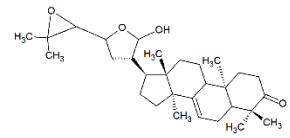
18	Tingenone	256	-10.1	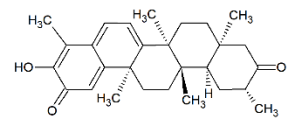
Control	NADPH	-	-10.0	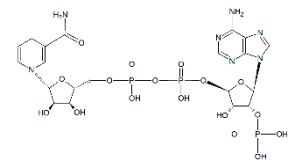

inhibitory potencies by interacting with a hydrophobic binding pocket of 5αR2.[53-55] Besides, ganoderic acid TR and DM from *Ganoderma lucidum* were reported to have inhibitory activities against 5αR2, and all these triterpenoids had a steroid ring skeleton with different side-chains at C-17.[56]

In the holo-5αR2, 5 amino acids (Tyr98, Leu100, Asn102, Arg168, and Arg171) were predicted to be involved in binding with testosterone. Surrounding regions of these amino acids were considered as predicted testosterone binding site. Among these 5 amino acids, Asn102 was identified to bind with testosterone via hydrogen bonding using UCSF Chimera. 247 out of 577 terpenes were calculated to have lower binding energies than testosterone (-6.3 kcal/mol) against its predicted binding site (Table 2). Namely, these 247 terpenes except monoterpenoids would be likely to have type B inhibitory activities. As the number of isoprene unit in backbone of terpenes increased, the proportion of terpenes predicted to have type B inhibitory activities within each terpene class tended to rise (Table 2). In addition, the binding energies of the two reference molecules, finasteride and dutasteride, against the predicted testosterone binding site were -6.2 kcal/mol and -8.1 kcal/mol, respectively. As compared with binding energies of testosterone, finasteride, and dutasteride, only 3 triterpenoids were calculated to have lower binding energies than testosterone, finasteride, and dutasteride against testosterone binding site of 5αR2 (Table 3). In this study, these 3 triterpenoids were named as compound T31900, compound T34389, and compound T3710, respectively. Compound T31900 and T34389 were also predicted to have both type A and B inhibitory activities. Interestingly, compound T31900, T34389, and T3710 were noticed to have a pentacyclic ring skeleton in common. So far, pentacyclic triterpenes have been reported to have various therapeutic effects including

Table 2. Characteristics of 247 terpenes predicted to have lower binding energies than testosterone (-6.3 kcal/mol) against 5α-reductase type 2

Terpene class	Number of compounds	Structural characteristics	Backbone structure
Monoterpenoids	0/31	-	2 isoprene units
Iridoids	7/44	Bicyclic ring or tricyclic ring	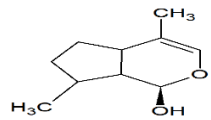
Sesquiterpenoids	2/112	Cyclopentapyranoid	3 isoprene units
Diterpenoids	38/124	Tricyclic ring or tetracyclic ring	4 isoprene units
Steroids	18/29	Steroid ring	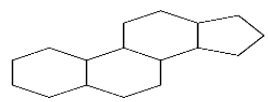
Triterpenoids	182/237	Steroid ring or pentacyclic ring	6 isoprene units

Table 3. Predicted binding energies (ΔG) and common structure of 3 triterpenoids predicted to have higher binding affinities than testosterone, finasteride, and dutasteride toward 5α-reductase type 2 (5αR2)

Compound	Compound T31900	Compound T34389	Compound T3710
Common structure			
Predicted binding affinities toward NADPH binding site of 5αR2			
ΔG (kcal/mol)	-10.2	-10.4	-8.2
Predicted binding affinities toward testosterone binding site of 5αR2			
ΔG (kcal/mol)	-8.7	-8.3	-8.2

inhibition of 5αR2 activity.[57-59] For example, ursolic acid, a pentacyclic triterpenoid acid, and bark extract of *Pygeum africanum* containing ursolic acid derivatives were reported to be effective in treatment of BPH by inhibiting 5αR2 activity.[57,58] To the best of our knowledge, while several studies on developing plant extracts which contain terpenes and promote hair growth have been reported,[15-18] there is a lack of studies focusing on the inhibitory effect of an individual terpene, especially a pentacyclic triterpenoid, on 5αR2 activity, except the study on the inhibitory activity of ginsenoside R_0 against 5αR2.[17] Thus, it seems that predicted competitive inhibitory activities of compound T31900, T34389, and T3710 against 5αR2 are further needed to be validated by *in vitro* and *in vivo* assays. Moreover, since it is necessary to consider possibilities of terpenes to bind and inhibit other enzymes expressed in scalp in order to determine whether terpenes would have competitive inhibitory activities specific to 5αR2, additional docking simulations of terpenes to other enzymes in scalp would be needed.

CONCLUSION

In the present study, comparison of competitive inhibitory activities of individual compounds within the same terpene classes as well as between different terpene classes were conducted using molecular docking based on the predicted 3D structure of 5αR2. Among 577 terpenes of 6 classes, triterpenoids having a steroid ring or a pentacyclic ring skeleton with a side-chain at C-16 or C-17 were predicted to have competitive inhibitory activities against NADPH binding site of 5αR2. Notably, certain triterpenoids with a pentacyclic ring in backbone were predicted to have even higher competitive inhibitory activities than finasteride and dutasteride, active ingredients of medicines for AGA treatment, against testosterone binding site of 5αR2. The present study would provide basic quantitative data about the potent competitive inhibitory activities of terpenes, especially triterpenoids, against 5αR2.

REFERENCES

(1) Russell, D. W.; Wilson, J. D. Steroid 5α-reductase: two genes/two enzymes. *Annu. Rev. Biochem.* **1994**, 63, 25-61.

(2) Eicheler, W.; Happle, R.; Hoffmann, R. 5α-Reductase activity in the human hair follicle concentrates in the dermal papilla. *Arch. Dermatol. Res.* **1998**, 290, 126-132.

(3) Hoffmann, R. Male androgenetic alopecia. *Clin. Exp. Dermatol.* **2002**, 27, 373-382.

(4) Inui, S.; Itami, S. Molecular basis of androgenetic alopecia: from androgen to paracrine mediators through dermal papilla. *J. Dermatol. Sci.* **2011**, 61, 1-6.

(5) Semalty, M.; Semalty, A.; Joshi, G. P.; Rawat, M. S. M. Hair growth and rejuvenation: an overview. *J. Dermatol. Treat.* **2011**, 22, 123-132.

(6) Imperato-McGinley, J.; Guerrero, L.; Gautier, T.; Peterson, R. E. Steroid 5α-reductase deficiency in man: an inherited form of male pseudohermaphroditism. *Science* **1974**, 186, 1213-1215.

(7) Yim, E.; Nole, K. L. B.; Tosti, A. 5α-Reductase inhibitors in androgenetic alopecia. *Curr. Opin. Endocrinol. Diabetes Obes.* **2014**, 21, 493-498.

(8) Kanti, V.; Messenger, A.; Dobos, G.; Reygagne, P.; Finner, A.; Blumeyer, A.; Trakatelli, M.; Tosti, A.; del Marmol, V.; Piraccini, B. M.; Nast, A.; Blume-Peytavi, U. Evidence-based (S3) guideline for the treatment of androgenetic alopecia in women and in men-short version. *J. Eur. Acad. Dermatol. Venereol.* **2018**, 32, 11-22.

(9) Kaufman, K. D.; Olsen, E. A.; Whiting, D.; Savin, R.; DeVilez, R.; Bergfeld, W.; Price, V. H.; Neste, D. V.; Roberts, J. L.; Hordinsky, M.; Shapiro, J.; Binkowitz, B.; Gormley, G. J. Finasteride in the treatment of men with androgenetic alopecia. *J. Am. Acad. Dermatol.* **1998**, 39, 578-589.

(10) Roehrborn, C. G.; Boyle, P.; Nickel, J. C.; Hoefner, K.; Andriole, G. Efficacy and safety of a dual inhibitor of 5-alpha-reductase types 1 and 2 (dutasteride) in men with benign prostatic hyperplasia. *Urology* **2002**, 60, 434-441.

(11) Eun, H. C.; Kwon, O. S.; Yeon, J. H.; Shin, H. S.; Kim, B. Y.; Ro, B. I.; Cho, H. K.; Sim, W. Y.; Lew, B. L.; Lee, W.; Park, H. Y.; Hong, S. P.; Ji, J. H. Efficacy, safety, and tolerability of dutasteride 0.5 mg once daily in male patients with male pattern hair loss: a randomized, double-blind, placebo-controlled, phase III study. *J. Am. Acad. Dermatol.* **2010**, 63, 252-258.

(12) Olsen, E. A.; Hordinsky, M.; Whiting, D.; Stough, D.; Hobbs, S.; Ellis, M. L.; Wilson, T.; Rittmaster, R. S. The importance of dual 5α-reductase inhibition in the treatment of male pattern hair loss: results of a randomized placebo-controlled study of dutasteride versus finasteride. *J. Am. Acad. Dermatol.* **2006**, 55, 1014-1023.

(13) Harcha, W. G.; Martinez, J. B.; Tsai, T. F.; Katsuoka, K.; Kawashima, M.; Tsuboi, R.; Barnes, A.; Ferron-Brady, G.; Chetty, D. A randomized, active- and placebo-controlled study of the efficacy and safety of different doses of dutasteride versus placebo and finasteride in the treatment of male subjects with androgenetic alopecia. *J. Am. Acad. Dermatol.* **2014**, 70, 489-498.

(14) Trost, L.; Saitz, T. R.; Hellstrom, W. J. Side effects of 5-alpha reductase inhibitors: a comprehensive review. *Sex. Med. Rev.* **2013**, 1, 24-41.

(15) Datta, K.; Singh, A. T.; Mukherjee, A.; Bhat, B.; Ramesh, B.; Burman, A. C. *Eclipta alba* extract with potential for hair growth promoting activity. *J. Ethnopharmacol.* **2009**, 124, 450-456.

(16) Kim, S. C.; Kang, J. I.; Park, D. B.; Lee, Y. K.; Hyun, J. W.; Koh, Y. S.; Yoo, E. S.; Kim, J. A.; Kim, Y. H.; Kang, H. K. Promotion effect of acankoreoside J, a lupane-triterpene in *Acanthopanax koreanum*, on hair growth. *Arch. Phar. Res.* **2012**, 35, 1495-1503.

(17) Murata, K.; Takeshita, F.; Samukawa, K.; Tani, T.; Matsuda, H. Effects of ginseng rhizome and ginsenoside R_0 on testosterone 5α-reductase and hair re-growth in testosterone-treated mice. *Phytothera. Res.* **2012**, 26, 48-53.

(18) Choi, J. S.; Jung, S. K.; Jeon, M. H.; Moon, J. N.; Moon, W. S.; Ji, Y. H.; Choi, I. S.; Son, S. W. Effects of *Lycopersicon esculentum* extract on hair growth and alopecia prevention. *J. Cosmet. Sci.* **2013**, 64, 429-443.

(19) Meng, X. Y.; Zhang, H. X.; Mezei, M.; Cui, M. Molecular docking: a powerful approach for structure-based drug discovery. *Curr. Comput. Aided Drug. Des.* **2011**, 7, 146-157.

(20) Altschul, S. F.; Madden, T. L.; Schäffer, A. A.; Zhang, J.; Zhang, Z.; Miller, W.; Lipman, D. J. Gapped BLAST and PSI-BLAST: a new generation protein databases search programs. *Nucleic Acids Res.* **1997**, 25, 3389-3402.

(21) Berman, H. M.; Westbrook, Z.; Feng, G.; Gilliland, T. N.; Bhat, H.; Weissig, I. N.; Shindyalov, P. E.; Bourne. The protein data bank. *Nucleic Acids Res.* **2000**, 28, 235-242.

(22) Apweiler, R.; Bairoch, A.; Wu, C. H.; Barker, W. C.; Boeckmann, B.; Ferro, S.; Gasteiger, E.; Huang, H.; Lopez, R.; Magrane, M.; Martin, M. J.; Natale, D. A.; O'Donovan, C.; Redaschi, N.; Yeh, L. L. UniProt: the universal protein

knowledgebase. *Nucleic Acids Res.* **2004**, 32, 115-119.

(23) Roy, A.; Kucukural, A.; Zhang, Y. I-TASSER: a unified platform for automated protein structure and function prediction. *Nat. Protoc*. **2010**, 5, 725-738.

(24) Yang, J.; Yan, R.; Roy, A.; Xu, D.; Poisson, J.; Zhang, Y. The I-TASSER suite: protein structure and function prediction. *Nat. Methods* **2015**, 12, 7-8.

(25) Li, X.; Roberti, R.; Blobel, G. Structure of an integral membrane sterol reductase from *Methylomicrobium alcaliphilum*. *Nature* **2015**, 517, 104-107.

(26) Diver, M. M.; Pedi, L.; Koide, A.; Koide, S.; Long, S.B. Atomic structure of the eukaryotic intramembrane RAS methyltransferase ICMT. *Nature* **2018**, 553, 526-529.

(27) Wang, Y.; Xiao, J.; Suzek, T. O.; Zhang, J.; Wang, J.; Bryant, S. H. PubChem: a public information system for analyzing bioactivities of small molecules. *Nucleic Acids Res.* **2009**, 37, W623-W633.

(28) O'Boyle, N. M.; Banck, M.; James, C. A.; Morley, C.; Vandermeersch, T.; Hutchison, G. R. Open Babel: an open chemical toolbox. *J. Cheminformatics* **2011**, 3, 33.

(29) Pettersen, E. F.; Goddard, T. D.; Huang, C. C.; Couch, G. S.; Greenblatt, D. M.; Meng, E. C.; Ferrin, T. E. UCSF Chimera– a visualization system for exploratory research and analysis. *J. Comput. Chem.* **2004**, 25, 1605-1612.

(30) Laskowski, R. A.; MacArthur, M. W.; Moss, D. S.; Thornton, J. M. PROCHECK: a program to check the stereochemical quality of protein structures. *J. Appl. Crystallogr.* **1993**, 26, 283-291.

(31) Wiederstein, M.; Sippl, M. J. ProSA-web: interactive web service for the recognition of errors in three-dimensional structures of proteins. *Nucleic Acids Res.* **2007**, 35, W407-W410.

(32) Colovos, C.; Yeates, T. O. Verification of protein structures: patterns of nonbonded atomic interactions. *Protein Sci*. **1993**, 2, 1511-1519.

(33) Triballeau, N.; Acher, F.; Brabet, I.; Pin, J. P.; Bertrand, H. O. Virtual screening workflow development guided by the "receiver operating characteristic" curve approach. Application to high-throughput docking on metabotropic glutamate receptor subtype 4. *J. Med. Chem.* **2005**, 48, 2534-2547.

(34) Trott, O.; Olson, A. J. AutoDock Vina: improving the speed and accuracy of docking with a new scoring function, efficient optimization, and multithreading. *J. Comput. Chem.* **2010**, 31, 455-461.

(35) Gaulton, A.; Bellis, L. J.; Bento, A. P.; Chambers, J.; Davies, M.; Hersey, A.; Light, Y.; McGlinchey, S.; Michalovich D.; Al-Lazikani, B.; Overington, J.P. ChEMBL: a large-scale bioactivity database for drug discovery. *Nucleic Acids Res.* **2012**, 40, D1100-D1107.

(36) Mysinger, M. M.; Carchia, M.; Irwin, J. J.; Shoichet, B. K. Directory of useful decoys, enhanced (DUD-E): better ligands and decoys for better benchmarking. *J. Med. Chem.* **2012**, 55, 6582-6594.

(37) Tian, G.; Mook, R.; Moss, M. L.; Frye, S. V. Mechanism of time-dependent inhibition of 5α-reductases by Δ^1-4-azasteroids: toward perfection of rates of time-dependent inhibition by using ligand-binding energies. *Biochemistry* **1995**, 34, 13453-13459.

(38) Frye, S. V. Discovery and clinical development of dutasteride, a potent dual 5α-reductase inhibitor. *Curr. Top. Med. Chem.* **2006**, 6, 405-421.

(39) Valli, M.; Dos Santos, R. N.; Figueira, L. D.; Nakajima, C. H.; Castro-Gamboa, I.; Andricopulo, A. D.; Bolzani, V. S. Development of a natural products database from the biodiversity of Brazil. *J. Nat. Prod.* **2013**, 76, 439-444.

(40) Morris, G. M.; Huey, R.; Lindstrom, W.; Sanner, M. F.; Belew, R. K.; Goodsell, D. S.; Olson, A. J. AutoDock4 and AutoDock Tools4: automated docking with selective receptor flexibility. *J. Comput. Chem.* **2009**, 16, 2785-2791.

(41) Roy, A.; Xu, D.; Poisson, J.; Zhang, Y. A protocol for computer-based protein structure and function prediction. *J. Vis. Exp.* **2011**, 57, e3259.

(42) Popot, J. L.; Engelman, D. M. Membrane protein folding and oligomerization: the two-stage model. *Biochemistry* **1990**, 29, 4031-4037.

(43) Sun, J.; Xiang, H.; Yang, L. L.; Chen, J. B. A review on steroidal 5α-reductase inhibitors for treatment of benign prostate hyperplasia. *Curr. Med. Chem.* **2011**, 18, 3576-3589

(44) Wigley, W. C.; Prihoda, J. S.; Mowszosicz, I.; Mendonca, B. B.; New, M. I.; Wilson, J. D.; Russell, D. W. Natural mutagenesis study of the human steroid 5α-reductase 2 isozyme. *Biochemistry* **1994**, 33, 1265-1270.

(45) Ramakrishnan, C.; Ramachandran, G. N. Stereochemical criteria for polypeptide and protein chain conformations: II. allowed conformations for a pair of peptide units. *Biophys. J.* **1965**, 5, 909-933.

(46) Gunasekaran, K.; Ramakrishnan, C.; Balaram, P. Disallowed Ramachandran conformations of amino acid residues in protein structures. *J. Mol. Biol.* **1996**, 264, 191-198.

(47) Pal, D.; Chakrabarti, P. On residues in the disallowed region of the Ramachandran map. *Biopolymers* **2002**, 63, 195-206.

(48) Sippl, M. J. Knowledge-based potentials for proteins. *Curr. Opin. Struct. Biol.* **1995**, 5, 229-235.

(49) Mandrekar, J. N. Receiver operating characteristic curve in diagnostic test assessment. *J. Thorac. Oncol.* **2010**, 5, 1315-1316.

(50) Gohlke, H.; Klebe, G. Approaches to the description and prediction of the binding affinity of small-molecule ligands to macromolecular receptors. *Angew. Chem. Int. Ed. Engl.* **2002**, 41, 2644-2676.

(51) Aggarwal, S.; Thareja, S.; Verma, A.; Bhardwaj, T. R.; Kumar, M. An overview on 5α-reductase inhibitors. *Steroids* **2010**, 75, 109-153.

(52) Kenny, B.; Ballard, S.; Blagg, J.; Fox, D. Pharmacological options in the treatment of benign prostatic hyperplasia. *J. Med. Chem.* **1997**, 40, 1293-1315.

(53) Thareja, S. Steroidal 5α-reductase inhibitors: a comparative 3D-QSAR study review. *Chem. Rev.* **2015**, 115, 2883-2894.

(54) Kurup, A.; Garg, R.; Hansch, C. Comparative QSAR analysis of 5α-reductase inhibitors. *Chem. Rev.* **2000**, 100, 909-924.

(55) Kumar, R.; Kumar, M. 3D-QSAR CoMFA and CoMSIA studies for design of potent human steroid 5α-reductase inhibitors. *Med. Chem. Res.* **2013**, 105-114.

(56) Liu, J.; Kenji, K.; Shimizu, K.; Kondo, R. Structure-activity relationship for inhibition of 5α-reductase by triterpenoids isolated from *Ganoderma lucidum*. *Bioorg. Med. Chem.* **2006**, 14, 8654-8660.

(57) Shin, I. S.; Lee, M. Y.; Jung, D. Y.; Seo, C. S.; Ha, H. K.; Shin, H. K. Ursolic acid reduced prostate size and dihydrotestosterone level in a rat model of benign prostatic hyperplasia. *Food Chem. Toxicol.* **2012**, 50, 884-888.

(58) Pagano, E.; Laudato, M.; Griffo, M.; Capasso, R. Phytotherapy of benign prostatic hyperplasia. A minireview. *Phytother. Res.* **2014**, 28, 949-955.

(59) Jäger, S.; Trojan, H.; Kopp, T.; Laszczyk, M. N.; Scheffler, A. Pentacyclic triterpene distribution in various plants- rich sources for a new group of multi-potent plant extracts. *Molecules* **2009**, 14, 2016-2031.

국문초록

컴퓨터 시뮬레이션에 의한 Terpene류의 5α-Reductase Type 2에 대한 경쟁적 저해능 예측

김륜희

식품영양학과

서울대학교 대학원

5α-Reductase type 2 (5αR2)는 모낭에서 testosterone이 dihydrotestosterone (DHT)로 전환되는 반응의 촉매 역할을 한다. 체내에 DHT가 증가하면 남성형 탈모가 유발되는 것으로 알려져 있다. 따라서 DHT의 생성량을 조절하는 효소인 5αR2의 활성을 저해함으로써 탈모의 진행을 지연시킬 수 있다. 주로 사용되고 있는 탈모 치료제의 성분으로는 finasteride와 dutasteride가 있으며, 두 물질 모두 5αR2에 대한 경쟁적 저해능을 갖는 것으로 알려져 있다. 그러나 이 물질들을 장기 복용 시 성기능 관련 부작용이 발생할 수 있다고 보고된 바 있다. 또한, 천연물을 이용한 모발 성장 효능에 관한 연구도 이루어지고 있다. 현재까지 한련초, 섬오갈피나무 잎, 홍삼, 토마토 등에서 얻은 추출물들의 모발 성장 효능이 있다고 보고되어 있는데, 이러한 추출물들은 모두

terpene류 물질들을 함유한다. 따라서 본 연구에서는 컴퓨터 시뮬레이션인 분자도킹을 이용하여 어떤 terpene류 물질이 5αR2의 보조인자인 NADPH와 이 효소의 기질인 testosterone에 대한 경쟁적 저해능을 가질 수 있는지를 예측하고자 하였다.

분자도킹을 수행하기에 앞서, I-TASSER 웹서버를 이용하여 5αR2의 입체구조를 예측하였다. 이후 예측 구조 모델을 기반으로 분자도킹하는 과정의 신뢰성을 평가하기 위해 receiver operating characteristic curve 분석을 수행하였다. NuBBE 데이터베이스로부터 얻은 577개 terpene류(monoterpenoids, iridoids, sesquiterpenoids, diterpenoids, steroids, triterpenoids)를 AutoDock Vina를 이용하여 예측모델의 NADPH와 testosterone의 결합부위에 도킹하였다. 또한, 비교물질로서 finasteride와 dutasteride도 예측 구조 모델에 도킹하였다. 전체 577개 terpene류 물질들 중, 18개의 triterpenoid류 물질들이 NADPH의 결합에너지보다 더 낮은 결합에너지를 가질 것으로 예측되었다. 또한 전체 577개 terpene류 중 247개 물질이 testosterone의 결합에너지보다 더 낮은 결합에너지를 가질 것으로 예측되었다. 이 중에서도 3개의 triterpenoid류가 탈모치료제의 성분인 finasteride와 dutasteride의 결합에너지보다도 더 낮은 결합에너지를 가질 것으로 예측되었다. 본 연구에서는 분자도킹을 통해 terpene류 내 혹은 terpene류 간의 5αR2에 대한 경쟁적 저해능 차이를 예측 및 비교하였다. Steroid ring 혹은 pentacyclic ring을 기본 골격으로 가지는 triterpenoid류가 다른 terpene류보다 5αR2에 대한 경쟁적 저해능이 높을 것으로 예측되었다.

주요어: 5α-Reductase type 2; 탈모; 분자도킹; 경쟁적 저해; Triterpenoid

학번: 2017-29285